

A large one-time addition of organic soil amendments increased soil macroporosity but did not affect intra-aggregate porosity of a clay soil

Kimmo Rasa^{a,*}, Mika Tähtikarhu^b, Arttu Miettinen^c, Topi Kähärä^c, Risto Uusitalo^a, Jarmo Mikkola^b, Jari Hyväluoma^{a,d}

^a Natural Resources Institute Finland, Tietotie 4, Jokioinen, FI-31600, Finland

^b Natural Resources Institute Finland, Latokartanonkaari 7-9, Helsinki, Finland

^c Department of Physics, Nanoscience Center, and School of Resource Wisdom, University of Jyväskylä, P.O. Box 35, Jyväskylä FI-40014, Finland

^d Häme University of Applied Sciences, Mustialantie 105, Mustiala 31310, Finland

ARTICLE INFO

Keywords:

Soil structure
Clay soil
Organic soil amendments
X-ray tomography
Aggregate
Helium ion Microscope

ABSTRACT

Soil structure is a dynamic property which controls a wide range of soil functions and is closely linked with soil carbon content. The carbon contents of agricultural soils are subject to several ongoing trends, including declining carbon stocks and attempts to increase the soil carbon reserves. In this study, we aimed to quantify how organic soil amendments, which have been shown to reduce long-term nutrient loads from agricultural fields, can impact soil structure. The structural impacts of a large one-time addition (8 tons carbon per hectare, three different soil amendments) of pulp and paper mill side stream sludges to a boreal clay soil were explored quantitatively in aggregate (X-ray microtomography, sample size 1–2 mm), core (water retention measurements, sample size 195 cm³) and column (macropores $\geq 80 \mu\text{m}$, sample size $\sim 20 \text{ dm}^3$) scales. Our results showed no micrometer-scale structural changes within soil aggregates despite the large number (25 aggregate per treatment) of imaged samples. However, the organic soil amendments had a statistically significant impact on the macroporosity. The macroporosity was on average 20–27 % higher compared to the control samples and visible even five years after the application of the amendments. Such change in soil structure improves soil aeration and fast infiltration of water during wet periods and extreme rain events and may thereby also reduce erosion risk by decreasing surface runoff. The increased microporosity was visible only in the column scale. No statistically significant differences were observed in the fraction of large pores in core scale water retention measurements. Probing the soil structural changes in macropore regime by X-ray tomography or developing sub-micron scale analysis methods are recommended approaches to improve our understanding of clay soil's structural changes induced by organic soil amendments.

1. Introduction

Soil structure, the three-dimensional organization and arrangement of solids and voids within the soil (Ghezzehei, 2012), is a dynamic property which controls physical, chemical, and biological processes in soils (Ghezzehei, 2012, Rabot et al., 2018, Johannes et al., 2019). The structure is affected by natural and anthropogenic processes, including moisture dynamics, tillage operations and usage of soil amendments. Organic matter and related microbe-derived compounds have been identified to have a key role in the formation and stabilization of soil structure (Hoffland et al., 2020, Costa, Raaijmakers, and Kuramae, 2018, Peele and Beale, 1941). The balance between accumulation and

respiration of organic carbon in agricultural soils has implications on climate regulation as well as the fertility and structure of soils (e.g. Schmidt et al., 2011, Lal, 2004, Hemingway et al., 2019). Moreover, currently the organic carbon stocks in agricultural soils are largely decreasing (e.g. Lal, 2004, Heikkinen et al., 2013), which highlights the importance of understanding how changes in soil organic matter content can affect soil structure and consequently soil functions.

Globally large quantities of various organic amendments are available (Thangarajan et al., 2013) which highlights the motivation to study their potential benefits in agricultural context. For example, organic fiber sludges derived from pulp and paper industry provides a potentially feasible possibility to amend carbon to soils, as they have been

* Corresponding author.

E-mail address: Kimmo.rasa@luke.fi (K. Rasa).

<https://doi.org/10.1016/j.still.2024.106139>

Received 12 January 2024; Received in revised form 25 April 2024; Accepted 1 May 2024

Available online 16 May 2024

0167-1987/© 2024 The Author(s). Published by Elsevier B.V. This is an open access article under the CC BY license (<http://creativecommons.org/licenses/by/4.0/>).

demonstrated to improve soil structure and reduce erosion and nutrient leaching from agricultural fields (Rasa et al., 2021, Rätty et al., 2023). It has been well demonstrated that typically the majority of the amended organic matter respire in few years (e.g. Zibilske et al., 2000, Foley and Cooperband, 2002, Rasa et al., 2021), while part of the organic matter can be persistent and affect soil structure for at least decades (e.g. Heikkinen et al., 2021, Vogel et al., 2014). While the impacts of soil organic carbon content on soil structure and preferential flow processes have been previously documented (Larsbo et al., 2016, Koestel and Jorda, 2014, Jarvis et al., 2007), the structural impacts of different types of organic soil amendments have been studied less. Organic soil amendments are often applied in relatively large doses and therefore their structural impacts can be expected to differ from the impacts of organic matter derived from natural processes.

Soil structure can be described with several different parameters describing the arrangement of solids and voids in the soil. This pore structure arrangement can vary from submicron (e.g. Guo et al., 2020) and aggregate scale (e.g. Yu et al., 2016) to macropores (Larsbo et al., 2016). While conventional laboratory and field methods for soil characterization give only indirect information about soil structure, X-ray microtomography (e.g. Hyväluoma et al., 2012, Jarvis et al., 2017, Pöhlitz et al., 2019, Zhang et al., 2023) enable explicit investigation of the soil pore system. Intra-aggregate porosity of soil aggregates has been previously imaged in several studies (e.g. Yu et al., 2016, Winstone et al., 2019, Peng et al., 2022, Gao et al., 2022). Some studies have shown significant changes in imaged pore structure due to contrasting climate conditions and soil management, such as drying-wetting (Ma et al., 2015) and freezing-thawing cycles (Ma et al., 2021, Liu et al., 2023), or tillage practices (Gao et al., 2022, Bacq-Labreuil, 2018). On the other hand, some investigations did not report differences in intra-aggregate porosity between contrasting treatments such as the application of structural lime (Bölscher et al., 2021) or biochar (Heikkinen et al., 2019). These examples show that X-ray tomography is an effective method to quantify changes, if any, in intra-aggregate structure caused by contrasting soil management. Tomography studies are, however, always limited by imaging resolution and sample size and can therefore probe only a certain part of the pore space. Therefore, a comprehensive study on soil structure can benefit from combining tomography analysis with soil column and core scale water retention studies. Soil pore properties can be spatially heterogeneous, and thus length scale of observation can affect related analyses (e.g. Koestel and Jorda, 2014). Column scale studies can reveal information which is not described by smaller-scale analyses. To understand structural changes induced by organic amendments, it would be beneficial to study the changes in different scales.

The aim of this study was to analyze soil structural changes induced by a large one-time addition of organic amendments to a clay soil. The present study was motivated by a recent field scale study by Rasa et al. (2021), in which ca. 8 Mg ha⁻¹ carbon was applied in the form of pulp and paper mill sludges on soil susceptible to erosion. In rainfall simulations, pulp and paper mill sludges were found to lower the tendency for particle detachment, which was attributed to direct interactions of soil minerals with the added particulate organic matter and/or microbe-derived compounds that stabilize soil aggregates (Rasa et al., 2021). In that study, indirect evidence of changes in soil structure was reported over the four-year study period. Thus, the hypothesis of the present study was that organic soil amendments induce changes in soil structure and those changes can be observed by using several complementary research methods in different length-scales. More specifically, organic soil amendments were expected to increase the inter-aggregate macroporosity of the soil. However, whether soil amendment induces changes in micrometer-scale pore structure within aggregates, or what would be the direction of possible changes, was unforeseeable. Overall, the present study provides fundamental knowledge on the impacts of pulp and paper mill sludges on a clay soil structure, which facilitates the recycling of industrial organic side streams into agriculture.

2. Material and methods

2.1. Field experiment and soil sampling

The field experiment was established at Jokioinen in south-west Finland in 2015 on a clay soil classified as a Luvic Stagnosol (Eutric, Clayic, Protovertic) (IUSS Working Group, 2015). The clay content of the soil was 47 %, the total C content was 2.3 % and the soil pH (H₂O) was 6.4. The experimental setup and the chemical quality of soil amendments have been described in detail elsewhere (Rasa et al., 2021). Briefly, three organic soil amendments 1) composted pulp mill sludge, 2) lime-stabilized pulp mill sludge, and 3) fiber sludge were applied in autumn 2015 at rates of 51, 52, and 72 Mg ha⁻¹ (Table 1; FIG S4c), respectively. The experiment layout was a randomized complete block design with five replicates (in total 20 plots, each measuring 6 m * 15 m). Unamended soil plots served as the control treatment. The field was growing wheat or oat in subsequent years. The depth of tillage in each autumn was approximately 10 cm.

Sampling for X-ray tomography and image analysis was conducted before cultivation in October 2020, i.e. five years after the application of soil amendments. Samples were collected by gently digging a bulk soil sample from the depth of 2.5–7.5 cm. Samples were taken from three locations and combined as one bulk sample per plot. In the laboratory, air-dried soil samples were gently sieved to collect 1–2 mm aggregates for X-ray tomography. From each plot, 5 aggregates were imaged with X-ray tomography, resulting in 25 aggregates for each treatment and 100 aggregates in total.

At the same time in October 2020, samples for soil moisture characteristics were taken from each plot to steel cylinders (height c. 4.8 cm, diameter c. 7.2 cm, 195 cm³, 2 replicates from each plot resulting in 10 samples per treatment, 40 samples in total) from the depth of 2.5–7.5 cm. The bottom of the cylinder was prepared in the field and lids were placed to preserve sample moisture. Samples were stored at +4 °C prior to analyses.

For the column scale experiments (rainfall simulation tests), one large undisturbed soil column (~20 dm³ soil) per plot (20 samples each year) was extracted from each field plot in sections of polyvinyl chloride sewage pipe (diameter 30 cm, height 40 cm), using a tractor-driven soil auger. Sampling was repeated in five consecutive springs (Ma 2016–Ma 2020). Samples were stored at +4 °C.

2.2. Drainage of large macropores

The data for the macroporosity in column-scale was derived from previous rainfall simulation test studies conducted by Rasa et al. (2021), see Supporting material) and supplemented in the present study with fifth year data. The rainfall simulation procedure has been described in detail in Uusitalo et al. (2012). Briefly, the bottom of the large undisturbed soil monoliths was prepared using a spatula to expose intact natural ped surfaces. The monoliths were then saturated from below during 1 d, maintained at saturation for an additional 2 d, and allowed to drain overnight. The volume of the drained amount of water from each monolith was measured. Water that can be gravitationally drained from

Table 1

Dry matter content (DM) of the three pulp and paper mill side streams used as soil amendments, and the amount of organic matter (OM), carbon (C), total nitrogen (N), total phosphorus (P), potassium (K), sulfur (S), and calcium (Ca) supplied to soil with the amendments. CPMS = composted pulp mill sludge, LPMS = lime-stabilized pulp mill sludge, FS = fiber sludge.

	DM %	OM ---Mg ha ⁻¹ ---	C -----	Tot-N -----	P -----	K -----	S -----	Ca -----
				kg ha ⁻¹				
CPMS	43.4	14.3	7.8	211	45	39	109	949
LPMS	49.7	17.3	9.0	253	53	30	131	2181
FS	33.5	15.7	8.4	13	2	1	7	2269

the monoliths induced a maximum suction of 0.4 m (water outlet pipe at the level of column bottom), which corresponds to the macroporosity (approximately $\geq 80 \mu\text{m}$) in the monoliths.

2.3. Measurements of soil moisture characteristics curve and soil shrinkage

Moisture retention curves were measured in suction pressures of 0.1, 0.3, 1.0, 3.2, 6.3, 10.0, 31.6, 63.1, 100.0, 316.2, 1585 (wilting point) and 39811 kPa. We used a sandbox apparatus (Eijkelkamp) at pressures ≤ 10 kPa. Ceramic plates in a pressure extractor were used in steps 31–320 kPa. We measured moisture contents in 1585 and 39811 kPa by vapor pressure equilibrium with saturated ammonium oxalate ($(\text{NH}_4)_2\text{C}_2\text{O}_4$) and sodium chloride (NaCl) solution, respectively. A 1.0 g portion of air-dried and sieved (a 5-mm sieve) soil sample was placed in a desiccator containing a saturated solution of the above-mentioned salts. The samples were allowed to equilibrate for 21 days and after weighing, dried overnight in a forced oven at 105 °C and weighed again. During each suction pressure step (0.1–320 kPa), we also measured shrinkage of the soil samples (vertical shrinkage with a Vernier caliper and horizontal shrinkage with a feeler gauge). Moisture contents were calculated as a share of soil water volume from the volume of the shrunk soil. We also analyzed changes in agronomically relevant soil moisture variables, including drainable moisture (0.1–10 kPa), easily plant available water (10–316 kPa), plant available water (10–1585 kPa) and porosity. Pore diameters corresponding with each suction pressure step were described with the Young–Laplace equation (e.g. Turunen et al., 2020).

2.4. X-ray microtomography imaging of intra-aggregate pore structure

From each of the 20 plots, five soil aggregates of 1–2 mm in diameter were randomly chosen for X-ray imaging for a total of 100 samples. The aggregates were embedded in epoxy glue and placed either on top of, or in a hole drilled through, a carbon fiber rod. The resulting samples were then imaged using Xradia MicroXCT-400 tomograph (Xradia, Concord, California, USA). The required field of view for imaging the whole aggregates was approximately 8 mm^3 resulting in a voxel size of approximately $2.3 \mu\text{m}$. The X-ray source was set to 40 kV acceleration voltage, 4 W X-ray tube power and the beam was filtered through a 0.20 mm thick glass filter. Each scan consisted of 941 radiographs taken over 188 degrees of rotation with an 8 s exposure time each. Three dimensional volumetric images with 992^3 voxels were reconstructed from the radiographs using a filtered back projection algorithm (Feldkamp et al., 1984).

The processing of the reconstructed images started by applying a 3D median filter (Gonzalez and Woods, 2002) with a 2-voxel radius to reduce imaging noise (Fig. 1). After this, voids were separated from the solid phase by segmenting the images using the Otsu method (Otsu, 1979). Small, non-physical pores created by imaging noise were removed by classifying pore regions less than 30 voxels ($365 \mu\text{m}^3$) in volume as part of the solid phase. Similarly, small solid regions created from imaging noise, and larger solid regions detached from the main aggregate were removed by classifying solid regions less than 100 000 voxels (0.0012 mm^3) in volume as part of the void phase. The correspondence between the segmentations and the original reconstructions was checked manually.

To distinguish surface-connected pores and the void surrounding the aggregate, the interior pores were defined as the part of the void phase that is separated from the outside by capillary pores, i.e., pores that retain water against gravity. Capillary pores were defined to be those with a diameter of $30 \mu\text{m}$ or less (Madison, 2008). This translates to roughly 13 voxels or less given our imaging resolution. In order to determine the local pore diameter, the local thickness map (Hildebrand and Rügsegger, 1997) was calculated for the void phase, resulting in a pore diameter estimate for each voxel in the void phase. Here, the

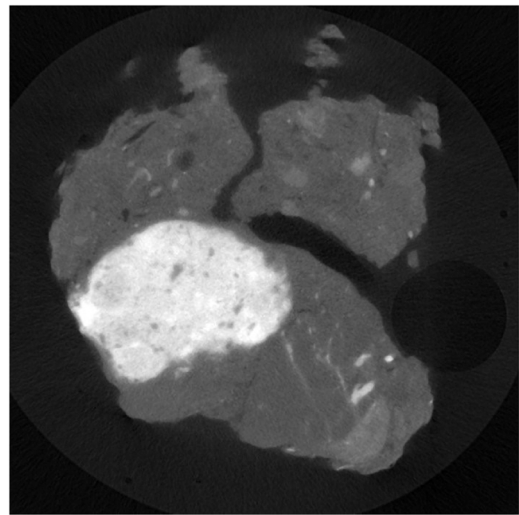


Fig. 1. An example of a median filtered 2D grayscale image of a soil aggregate. Around the aggregate, a layer of epoxy glue with some trapped air is also faintly visible.

diameter estimate for a voxel corresponds to the diameter of the largest sphere that fits entirely into the void phase and contains the voxel. The interior pore segmentation was then made with a flood fill (Gonzalez and Woods, 2002) operation on the local thickness map. The flood fill operation was started from void voxels at the edges of the image (i.e., locations that are surely outside of the aggregate), and the fill propagated through voxels whose local thickness value was larger than 13 voxels. The filled space was interpreted as exterior void, and the non-filled void phase as interior pores.

The outer surface layer of the aggregate was usually incorrectly classified as a part of the interior pores, but this effect was mitigated by applying a dilation operation (Gonzalez and Woods, 2002) with 1 voxel radius, to the voxels classified as exterior void space, effectively expanding the exterior void towards the aggregate by 1 voxel. Then, the voxels in the expanded exterior void were removed from the interior pores. To illustrate the result of this procedure a compound image, with the interior pores marked in red, the solid phase in white and the exterior void in black, is shown in Fig. 2.

The total porosity of each sample was calculated by dividing the number of voxels classified into the interior pore phase by the total

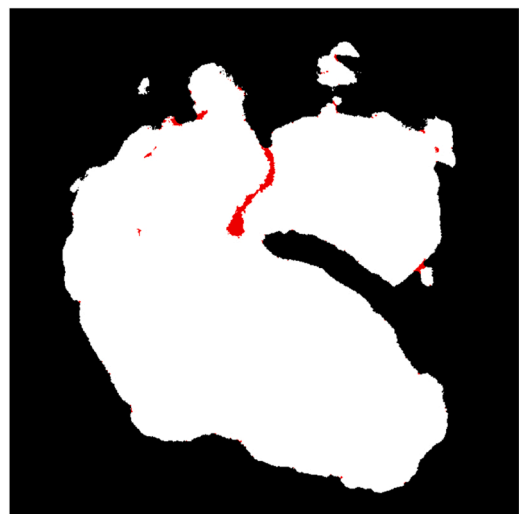


Fig. 2. Segmented 2D image of a soil aggregate. Pores are shown in red, solids in white and exterior of the aggregate in black.

number of voxels in the aggregate (solid and interior pores). Additionally, the fraction of interior pores accessible from the outside of the aggregate was determined. To this end, a flood fill was initiated from the exterior void voxels and let to propagate to the interior pore voxels. The number of voxels filled was divided by the total number of interior pore voxels to end up in the fraction of pores accessible from outside of the aggregate.

Pore depth was defined as the shortest distance from an interior pore voxel to the outside of the aggregate. This value was calculated for all the interior pore voxels using a seeded (geodesic) distance map algorithm (Soille, 2004). The outside of the particle was used as a set of seeds, and the algorithm was allowed to propagate only in the interior pores. The resulting distance map was statistically binned to estimate the pore depth distribution, and the corresponding mean and standard deviation were determined.

In order to quantify the sizes of the interior pores, the local thickness map of the interior pore space was statistically binned to estimate the pore diameter distribution and the average pore diameter, and its standard deviation were determined. To quantify how well accessible the interior pores are, porosity and pore depth were determined for the fraction of interior pore space that was accessible by a small sphere of specific size. To this end, a flood fill was initiated from exterior void voxels, and let to propagate into those interior pore voxels whose corresponding local thickness value was more than the selected sphere diameter. Local thickness and pore depth statistics were determined from the filled voxels. Sphere sizes in the range of 3–30 μm were tested, resulting in both pore diameter and pore depth statistics as a function of size.

Reconstructions and image analysis were made using pi2 (freely available at <https://github.com/arttumiainen/pi2>), NumPy (Harris et al., 2020), and Scikit-Image (van der Walt et al., 2014) software packages.

2.5. Statistical analysis

The micrometer-scale porosity data set from X-ray microtomography analyses incorporated variables for two pore size classes (pore size greater or lesser than 30 μm), porosity (quotient of void volume and total volume) and accessible porosity (fraction of porosity accessible through surface pores). The core scale data contained four variables (drainable water, easily plant available water, plant available water, and porosity) and the shrinkage data included three different material volume share variables (at the pressures of 32 kPa, 100 kPa and 320 kPa). Finally, the column-scale data for the macroporosity consisted of yearly repeated measurements from 2016 to 2020.

Treatment effects other than the macropore variables were tested by using the one-way analysis of variance (one-way ANOVA) and the values with each three treatments of interest were tested against the control level by using the contrasts. The main statistical emphasis in these ANOVA tests was on finding a suitable distribution or a transformation for each variable that did not seem normally distributed. More complex analysis was required for the macroporosity that was measured repeatedly during a five-year period. The effects of the treatments on this variable were tested by specifying contrasts in a repeated measures mixed-effects model.

Shrinkage variables could be treated as normally distributed despite the limits of the variation ([0,1]) and all the moisture variables could be assumed to follow the beta distribution. The ANOVA analysis of the porosity variables, however, was somewhat more complicated as these variables had to be transformed by applying either arcsine, logit or log transformation. All the mentioned distributions and transformations resulted in statistically reasonably well-behaving variables and normally distributed residuals (Anderson-Darling test).

For the repeated measures mixed effects model (the macroporosity 2016–2020), the final test model contained the year and the treatment variables as fixed effects, while the interaction term (year * treatment)

turned out to be insignificant. As the other covariance structure candidates did not converge in the estimations, the covariance structure for the repeated measurements was selected by comparing the information criteria values from the model with the autoregressive structure with lag one and from the model with the structure of compound symmetry. The autoregressive structure was chosen for the final model. The variance for the year 2017 seemed bigger than the variance for the other years, but the homogeneity of the covariance parameters across the years was confirmed by the likelihood ratio test (COVTEST option in GLIMMIX), and according to the estimations and the significance tests, other random effects were not considered necessary for the model. Approximate degrees of freedom and the bias correction for the test statistics were calculated by using the improved Kenward and Roger (2009) method.

All the testing was done by using the GLIMMIX procedure (from the SAS program's STAT module version 15.2, SAS Institute Inc., Cary, NC, USA).

3. Results

3.1. Macropores

The macroporosity in the large soil columns varied between 7.0 % and 9.3 % (Fig. 3), and the control treatment differed from all of the studied treatments ($p < 0.01$). The mean macroporosity was 7.0 % in the control columns and 8.5–9.3 % in the treatments. Although the level of macroporosity differed significantly between the years ($p < 0.0001$), there was no significant interaction between the year and treatment ($p = 0.1165$), which indicates that the differences between the treatments (studied materials and control) showed a similar trend over the study time (Supplement1).

3.2. Soil moisture characteristics and shrinkage

The measured core scale (195 cm³) volumetric soil moistures varied between 0.55 and 0.03 in the studied pressure range (Fig. 4). The moisture value ranges in the different materials largely overlapped in all pressure steps (Fig. 4). Regarding the agronomically relevant soil moisture variables (drainable moisture, easily plant available water and plant available water) and porosity, we found no statistically significant differences between the materials ($p \geq 0.28$). Only minor shrinkage during the drying was observed (0.02–0.03 V/V) and there were no statistically significant differences ($p \geq 0.29$) regarding the shrinkage of

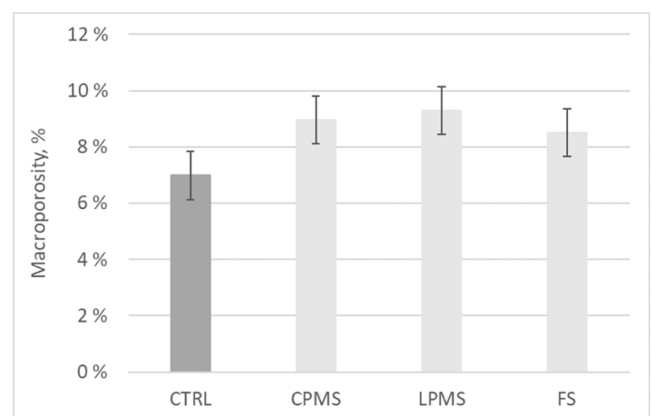


Fig. 3. The macroporosity in unamended control soil (CTRL) and soils amended with composted pulp mill sludge (CPMS), lime-stabilized pulp mill sludge (LPMS) and fiber sludge (FS) during the time period 2016–2020 in the column scale drainage experiment (data pooled over 5 years research period). The bars denote the 95 % confidence intervals. Data for individual years presented in Supplement 1 (Fig. S1).

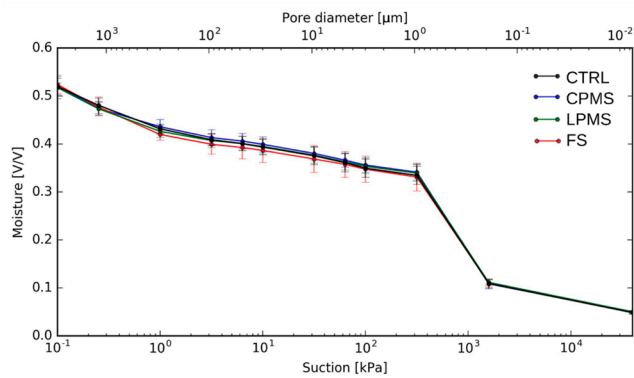


Fig. 4. Measured core scale mean moisture contents in different suction pressures in unamended control soil (CTRL) and soils amended with composted pulp mill sludge (CPMS), lime-stabilized pulp mill sludge (LPMS) and fiber sludge (FS). The error bars show standard deviations.

soils amended with the studied materials. Data for these additional analyses are presented in Supplement 2.

3.3. Intra-aggregate pore space characterization

Reconstructed images from X-ray tomography allowed visualization and quantitative analysis of the segmented aggregate structure and the internal pore network (Fig. 5). Aggregate mean porosities of different treatments derived from X-ray tomography images varied between 0.018 and 0.025 and the highest and lowest observed porosity in individual samples were 0.072 and 0.004, respectively. Variations within treatments were high (0.011–0.014) compared to relatively small differences between the mean porosities of different treatments. No statistically significant differences between treatments were observed ($p > 0.60$) despite the high number of replicate samples imaged in this study (25 samples for each treatment, 100 samples in total). The pore size distributions for each treatment are shown in Fig. 6. There was high spatial variation regarding the distribution of the pore spaces within the samples (Fig. 5). These distributions appear very similar for each treatment, and approximately half of the porosity was in pore size class $< 10 \mu\text{m}$. Pore size distributions were tested statistically by considering two pore size classes, i.e., pores with diameters greater or lesser than $30 \mu\text{m}$, but no statistically significant differences were observed ($p > 0.12$). Furthermore, imaged pore spaces were analyzed for pore accessibility and pore depth and these analyses did not reveal any statistically significant differences between treatments. Data for these additional analyses are presented in Supplement 3.

4. Discussion

Our results showed that among the studied soil structure variables,

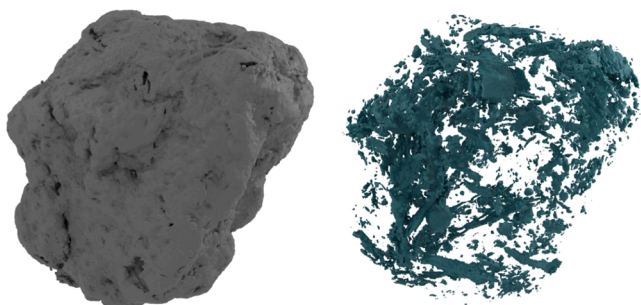


Fig. 5. A representative visualization of the shape of the 3D-imaged soil aggregate (left) and the pore spaces ($> 2 \mu\text{m}$) within the aggregate (right).

the effect of organic soil amendments (pulp and paper industry side-streams) was visible only in the macroporosity ($\geq 80 \mu\text{m}$) at the largest column scale used in the drainage experiments. Although the macroporosity varied between the years (Supplement 1), likely due to weather conditions during the preceding winters (Rasa et al., 2009, Rasa et al., 2021), all three studied soil amendments increased the macroporosity statistically significantly ($p < 0.05$) over the study period (5 yr.). In line with the present findings, Larsbo et al. (2016) showed in a field experiment how the share of large pores in the pore size class (200–600 μm) was greater in areas with high organic matter content whereas for pore sizes $> 600 \mu\text{m}$ they did not find a correlation with organic matter. Also, Koestel and Jorda (2014) as well as Jarvis et al. (2007) showed how organic matter content can affect preferential flow processes. The present column scale results support the hypothesis that soil amendments change pore structure by increasing the share, and likely also continuity, of the macropores. The latter could be further examined by X-ray tomography using a resolution suitable for the macropore regime. Nevertheless, drainage experiments suggest that the studied organic soil amendments show potential to improve soil water infiltration through macropores in clay soils. Increased infiltration can reduce surface runoff and prevent soil erosion and nutrient loading from arable land (Turtola et al., 2007).

Contrary to drainage experiments, the soil moisture characteristic measurements conducted with small core samples did not show statistically significant differences between the control and treatments ($p = 0.3$). Likely the inconsistency between the results of drainage and water retention measurements was caused by several factors. The core samples for water retention measurements were taken from the depth where the soil amendments were mixed (cultivation depth appr. 10 cm). In this soil layer possible changes in soil structure would have been expected to be the most pronounced, but on the other hand, soil structure is disturbed annually by cultivation. The large column scale experiment was conducted over 5 years (Fig. 3, pooled data over the experimental period), whereas the core scale measurements were done only in 2020. However, in the column scale, the macroporosity in amended treatments was 12–33 % higher in the last sampling year 2020 (five years after the amendment, Supplement 1) compared to non-amended control plots. Variation in factors such as soil drying and freezing cycles, and timing of tillage operations can cause interannual and seasonal dynamics in the studied structural parameters (Keskinen et al., 2019, Leuther and Schlüter, 2021). In addition, there is considerable spatial variation in the macroporosity (e.g. Pittman et al., 2020), which can be better captured with the large soil columns than with small soil samples. In previous studies (e.g. Koestel and Jorda, 2014) an impact of observation scale on measuring water flow in large pores has been noted too. These results underline the relevance of the spatial and temporal observation scale in the quantification of structural changes in spatially heterogeneous structured soils.

The effect of organic matter on soil water retention has been considered in several studies. While it is widely accepted that soil organic matter content influences the plant available water in soil, it is known that soil type and prevailing organic matter status influence how the change in organic matter content alters water retention (Rawls et al., 2003). Minasny and McBratney (2018) conducted a meta-analysis using global data consisting of over 50,000 measurements and arrived at the general conclusion that an increase in soil organic matter content has only a small effect on soil water retention. The effect appeared to be larger in coarser and lesser in finer soils. However, positive effects of soil organic matter on porosity responsible for storing plant-available water have been detected in some studies where the variation in soil organic carbon content has been clearly larger than the differences induced by the organic matter addition in the present study (Fukumasu et al., 2022; Kirchmann and Gerzabek, 1999; Jensen et al., 2020). In their study of long-term effects of organic amendments in a fine-textured Vertisol, Zhou et al. (2020) found that 33 years of application of straw and manure did not affect the retention of plant available water in the soil.

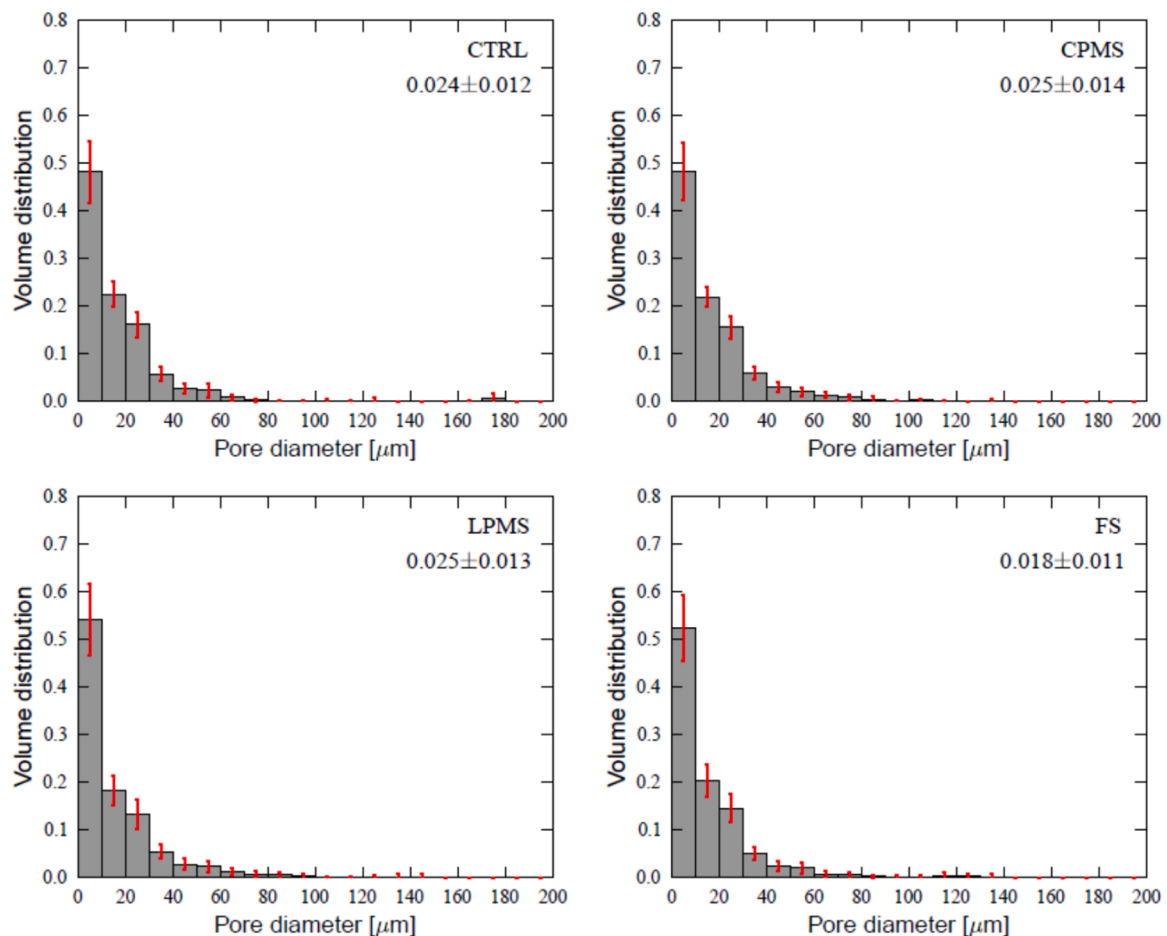


Fig. 6. Pore size distributions of aggregates for unamended control soil (CTRL) and soils amended with composted pulp mill sludge (CPMS), lime-stabilized pulp mill sludge (LPMS) and fiber sludge (FS). For each soil, shown are the mean volume distribution and standard deviation. The mean total imaged porosity and its standard deviation are shown for each treatment in the corresponding panel.

For Finnish clay soils, [Soinne et al. \(2023\)](#) did not find beneficial impacts of organic matter on water retention while organic matter content had a positive influence on macroporosity.

In the present work, we sampled a field experiment where differences in the organic matter quality were due to a single high dose of added external wood fiber-based organic soil amendment instead of native organic matter. Regardless, no difference in water retention properties between different treatments could be observed in the drying curves. This finding can be understood on the basis of previous investigations indicating that in clay soils the effect of additional organic matter has only a minor effect on water retention. Also, the differences in soil carbon content become less evident over time due to the microbiological decomposition of soil amendments. In the experimental field used in this study, soil carbon content four years after application was 0.18 percentage points higher in the CPMS (2.50 %) than in the control treatment (2.32 %, $p=0.053$), while differences between the other treatments were even smaller ([Rasa et al., 2021](#)). The direct soil sample-based measurement of soil carbon content is a relatively robust approach to study soil carbon dynamics. In a recent study, [Keskinen et al. \(2024\)](#) used the same experimental field to study soil carbon pools after the repeated application (applied in autumn 2020) of the soil amendments. There was an indication that wood fiber sludge treatment tended to increase the pool of mineral-associated organic carbon. The carbon associated with clay-sized soil particles is known to be more stable than free particulate organic carbon ([Baldock and Skjemstad, 2000](#)) and it can also contribute to the development of soil structure in a nanometer-scale.

The internal micrometer scale pore structure of soil aggregates was in the present work studied by X-ray tomography. Despite the large number of replicate samples imaged for each treatment, image analysis did not show differences in any quantified structural property. While X-ray tomography has turned out to be an effective method to study soil structure, the majority of work has concentrated on imaging of intact soil cores and so far, quite a limited number of studies have focused on the internal structure of aggregates (see also Introduction). Nevertheless, it has been shown that 3D imaging of aggregates is able to observe and quantify differences between aggregates from differently managed soils. Typically, aggregate structures have been imaged with a resolution of a few micrometers (e.g. [Gao et al., 2022](#), [Ma et al., 2021](#), [Peng et al., 2022](#)), which are comparable to the resolution used in our investigation. The aggregate porosities determined here (ca. 0.02) were comparable with those observed in previous studies, which have reported porosity values derived for clay soil aggregates (e.g., [Heikkinen et al., 2019](#), [Bölscher et al., 2021](#)). Thus, the absence of structural differences between amended soils and non-amended control soil indicates that high dose of studied organic amendments unlikely leads to long-term structural changes on the 1–2 mm aggregate level in arable clay soils in boreal conditions.

Resolution and sample size are always limited in 3D imaging studies. Therefore, imaging studies only probe a certain part of the pore space. It is thus possible that there are differences in the pore structure that are non-resolvable in tomographic images. Similarly, differences in inter-aggregate macroporosity indicated by drainage experiments cannot be evaluated when focusing on small sample size like the aggregates used in

the present study. As an example, the study by Bölscher et al. (2021) considering the effects of structural liming on clay soil structure found no difference in the intra-aggregate pore network, whereas changes in the macropore network were observed. The results from column scale experiments of the present study suggest that the larger scale X-ray tomography studies probing macropore networks could further improve the understanding of the structural changes induced by organic soil amendments.

The imaging resolution of the present study (2.3 μm voxel size) limits the observations to micrometer scale. However, in the submicron region mineral surfaces may play an important role in the accumulation of persistent microbe-derived organic matter (Kopittke et al., 2018, 2020). Also, structural features in submicron scale contribute to water retention in high suction pressures (>300 kPa), where all our samples retained a large share of water (Fig. 4, see also Supplement, which provides qualitative consideration on submicron scale observations based on Helium Ion Microscopy). Organic amendments have been found to increase water retention in the dry range of fine-textured soils (Zhou et al., 2020), while no such changes were observed in the present study. Increasing soil organic matter content can have counteracting influences on water retention under very dry conditions: additional functional groups may provide sorption sites for water molecules whereas organic matter associated with mineral surfaces may also cover and mask a notable fraction of the specific surface area of mineral particles (Kaiser and Guggenberger, 2003) or increase the subcritical water repellence of mineral surfaces (Ramirez-Flores et al., 2008).

The initial motivation of the present study was based on the results showing that the studied organic soil amendments significantly reduced erosion of the clay soil at least four years after application (Rasa et al., 2021). To deepen our understanding about the impacts of these organic soil amendments on clay soils, the present paper examined changes in soil structure and water retention properties in different length scales. It was found that soil structure was affected by soil amendments only in macropore scale. These large pores are responsible for soil aeration and fast water movements, which is likely beneficial for crop production in the boreal climate zone. More comprehensive studies on characteristics of soil structure at macropore and larger macro-aggregate scales are suggested using bigger sample size and lower X-ray tomography resolution methods (see e.g. Liu et al., 2023). On the other hand, aggregate-scale inspection (1–2 mm in diameter) showed no differences between the treatments. Therefore, a study of soil structural properties in sub-micrometer scale using quantitative 3D imaging methods such as X-ray nanotomography or high-resolution microscopy techniques could improve our understanding about interactions of soil particles and added organic matter, i.e. the nanometer scale phenomenon contributing to soil structural stability and preservation of soil carbon in recalcitrant form (organo-mineral associations). Sub-micrometer scale studies could also further clarify why studied organic soil amendments are capable to reduce soil erosion and nutrient leaching from clay soils (Rasa et al., 2021).

5. Conclusions

Impacts of a large single addition of organic soil amendments (8 tons C per hectare) on soil structure were explored in different scales using column scale observations, core scale water retention measurement and aggregate scale X-ray tomography. Among the studied variables, a statistically significant increase was found only regarding the macroporosity (≥ 80 μm) in column scale and the impact was visible five years after the application of the amendments. Such change in soil structure improves soil aeration and fast infiltration of water during wet periods and extreme rain events and may thereby also reduce erosion risk by decreasing surface runoff. Totally 100 soil aggregates were imaged and analyzed but no changes in micrometer scale pore characteristics were observed. To better quantify and understand changes in soil macropore regime, X-ray tomography using core and column scale samples would

be recommended.

CRediT authorship contribution statement

Kimmo Rasa: Writing – review & editing, Writing – original draft, Validation, Supervision, Resources, Project administration, Methodology, Investigation, Funding acquisition, Conceptualization. **Mika Tähtikarhu:** Writing – review & editing, Writing – original draft, Validation, Investigation, Formal analysis. **Jarmo Mikkola:** Writing – original draft, Validation, Methodology, Formal analysis. **Jari Hyväluoma:** Writing – review & editing, Writing – original draft, Visualization, Validation, Supervision, Software, Resources, Methodology, Investigation, Funding acquisition, Formal analysis, Conceptualization. **Risto Uusitalo:** Writing – review & editing, Investigation. **Arttu Miettinen:** Writing – review & editing, Visualization, Validation, Software, Methodology, Investigation, Funding acquisition, Formal analysis, Data curation, Conceptualization. **Topi Kähärä:** Visualization, Software, Investigation, Formal analysis.

Declaration of Competing Interest

The authors declare that they have no known competing financial interests or personal relationships that could have appeared to influence the work reported in this paper.

Data Availability

Data will be made available on request.

Acknowledgements

This study was funded by Maa- ja vesiteknikan tuki ry, Soil Improvement Fibers- and HiiletIn-projects funded by Ministry of Agriculture and Forestry of Finland (Ravinteiden kierrätyksen kekeiluohjelma and Catch the Carbon research and innovation programme), Ministry of the Environment (Water Protection Programme), and Tandem Industry Academia Professor funding by The Finnish Research Impact Foundation.

Appendix A. Supporting information

Supplementary data associated with this article can be found in the online version at doi:10.1016/j.still.2024.106139.

References

- Bacq-Labreuil, A., Crawford, J., Mooney, S.J., Neal, A.L., Akkari, E., McAuliffe, C., Zhang, X., Redmile-Gordon, M., Ritz, K., 2018. Effects of cropping systems upon the three-dimensional architecture of soil systems are modulated by texture. *Geoderma* 332, 73–83. <https://doi.org/10.1016/j.geoderma.2018.07.002>.
- Baldock, J.A., Skjemstad, J.O., 2000. Role of the soil matrix and minerals in protecting natural organic materials against biological attack. *Org. Geochem.* 31, 697–710. [https://doi.org/10.1016/S0146-6380\(00\)00049-8](https://doi.org/10.1016/S0146-6380(00)00049-8).
- Bölscher, T., Koestel, J., Etana, A., Ulén, B., Berglund, K., Larsbo, M., 2021. Changes in pore networks and readily dispersible soil following structure liming of clay soils. *Geoderma* 390, 114948. <https://doi.org/10.1016/j.geoderma.2021.114948>.
- Costa, O.Y.A., Raaijmakers, J.M., Kuramae, E.E., 2018. Microbial extracellular polymeric substances: ecological function and impact on soil aggregation. *Front. Microbiol.* 9, 1636. <https://doi.org/10.3389/fmicb.2018.01636>.
- van der Walt, S., Schönberger, J.L., Nunez-Iglesias, J., Boulogne, F., Warner, J.D., Yager, N., Gouillart, E., Yu, T., the scikit-image contributors, 2014. scikit-image: image processing in Python. *PeerJ* 2, e453. <https://doi.org/10.7717/peerj.453>.
- Feldkamp, L.A., Davis, L.C., Kress, J.W., 1984. Practical cone-beam algorithm. *J. Opt. Soc. Am. A* 1 (6).
- Foley, B.J., Cooperband, L.R., 2002. Paper mill residuals and compost effects on soil carbon and physical properties. *J. Environ. Qual.* 31, 2086–2095. <https://doi.org/10.2134/jeq2002.2086>.
- Fukumasu, J., Jarvis, N., Koestel, J., Kätterer, T., Larsbo, M., 2022. Relations between soil organic carbon content and the pore size distribution for an arable topsoil with large variations in soil properties. *Eur. J. Soil Sci.* 73, e13212 <https://doi.org/10.1111/ejss.13212>.

- Gao, Y., Liang, A., Fan, R., Guo, Y., Zhang, Y., McLaughlin, N., Chen, X., Zheng, H., Wu, D., 2022. Quantifying influence of tillage practices on soil aggregate microstructure using synchrotron-based micro-computed tomography. *Soil Use Manag.* 38, 850–860. <https://doi.org/10.1111/sum.12755>.
- Ghezzehei, T.A., 2012. Soil structure. In P.M. Huang, Y. Li, & M.E. Sumner (Eds.), *Handbook of Soil Sciences: Properties and Processes*. CRC Press, pp. 1–18. <https://doi.org/10.1201/b11267>.
- Gonzalez, R.C., Woods, R.E., 2002. *Digital Image Processing, 2 edition*. Prentice-Hall.
- Guo, L., Shen, J., Li, B., Li, Q., Wang, C., Guan, Y., D'Acqui, L.P., Luo, Y., Tao, Q., Xu, Q., Li, H., Yang, J., Tang, X., 2020. Impacts of agricultural land use change on soil aggregate stability and physical protection of organic C. *Sci. Total Environ.* 707, 136049. <https://doi.org/10.1016/j.scitotenv.2019.136049>.
- Harris, C.R., Millman, K.J., van der Walt, S.J., et al., 2020. Array programming with NumPy. *Nature* 585, 357–362. <https://doi.org/10.1038/s41586-020-2649-2>.
- Heikkinen, J., Keskinen, R., Soinne, H., Hyväluoma, J., Nikama, J., Wikberg, H., Källi, A., Siipola, V., Melkior, T., Dupont, C., Campargue, M., Larsson, S.H., Hannula, M., Rasa, K., 2019. Possibilities to improve soil aggregate stability using biochars derived from various biomasses through slow pyrolysis, hydrothermal carbonization, or torrefaction. *Geoderma* 344, 40–49. <https://doi.org/10.1016/j.geoderma.2019.02.028>.
- Heikkinen, J., Ketoja, E., Nuutinen, V., Regina, K., 2013. Declining trend of carbon in Finnish cropland soils in 1974–2009. *Glob. Chang. Biol.* 19, 1456–1469. <https://doi.org/10.1111/gcb.12137>.
- Heikkinen, J., Ketoja, E., Seppänen, L., Luostarinen, S., Fritze, H., Pennanen, T., Peltoniemi, K., Velmala, S., Hanajik, P., Regina, K., 2021. Chemical composition controls the decomposition of organic amendments and influences the microbial community structure in agricultural soils. *Carbon Manag.* 12, 359–376. <https://doi.org/10.1080/17583004.2021.1947386>.
- Hemingway, J.D., Rothman, D.H., Grant, K.E., Rosengard, S.Z., Eglinton, T.I., Derry, L.A., Galy, V.V., 2019. Mineral protection regulates long-term global preservation of natural organic carbon. *Nature* 570, 228–231. <https://doi.org/10.1038/s41586-019-1280-6>.
- Hildebrand, T., Rüegsegger, P., 1997. A new method for the model-independent assessment of thickness in three-dimensional images. *J. Microsc.* 185, 67–75. <https://doi.org/10.1046/j.1365-2818.1997.1340694.x>.
- Hoffland, E., Kuyper, T.W., Comans, R.N.J., Creamer, R.E., 2020. Eco-functionality of organic matter in soils. *Plant. Soil.* 455, 1–22. <https://doi.org/10.1007/s11104-020-04651-9>.
- Hyväluoma, J., Thapaliya, M., Alaraudanjoki, J., Sirén, T., Mattila, K., Timonen, J., Turtola, E., 2012. Using microtomography, image analysis and flow simulations to characterize soil surface seals. *Comput. Geosci.* 48, 93–101. <https://doi.org/10.1016/j.cageo.2012.05.009>.
- IUSSWorking Group. (2015). *International Soil Classification System for Naming Soils and Creating Legends for Soil Maps*. Rome: FAO.
- Jarvis, N., Larsbo, M., Koestel, J., 2017. Connectivity and percolation of structural pore networks in a cultivated silt loam soil quantified by X-ray tomography. *Geoderma* 287, 71–79. <https://doi.org/10.1016/j.geoderma.2016.06.026>.
- Jarvis, N., Larsbo, M., Roulier, S., Lindahl, A., Persson, L., 2007. The role of soil properties in regulating non-equilibrium macropore flow and solute transport in agricultural topsoils. *Eur. J. Soil Sci.* 58, 282–292. <https://doi.org/10.1111/j.1365-2389.2006.00837.x>.
- Jensen, J.L., Schjøning, P., Watts, C.W., Christensen, B.T., Munkholm, L.J., 2020. Short-term changes in soil pore size distribution: impact of land use. *Soil Tillage Res.* 199, 104597. <https://doi.org/10.1016/j.still.2020.104597>.
- Johannes, A., Weisskopf, P., Schulin, R., Boivin, P., 2019. Soil structure quality indicators and their limit values. *Ecol. Indic.* 104, 686–694. <https://doi.org/10.1016/j.ecolind.2019.05.040>.
- Kaiser, K., Guggenberger, G., 2003. Mineral surfaces and soil organic matter. *Eur. J. Soil Sci.* 54, 219–236. <https://doi.org/10.1046/j.1365-2389.2003.00544.x>.
- Kenward, M.G., Roger, J.H., 2009. An improved approximation to the precision of fixed effects from restricted maximum likelihood. *Comput. Stat. Data anal.* 53, 2583–2595. <https://doi.org/10.1016/j.csda.2008.12.013>.
- Keskinen, R., Nikama, J., Kostensalo, J., Rätty, M., Rasa, K., Soinne, H., 2024. Methodological choices in size and density fractionation of soil carbon reserves – a case study on wood fiber sludge amended soils. *Heliyon* 10, e24450. <https://doi.org/10.1016/j.heliyon.2024.e24450>.
- Keskinen, R., Rätty, M., Kaseva, J., Hyväluoma, J., 2019. Variations in near-saturated hydraulic conductivity of arable mineral topsoils in south-western and central-eastern Finland. *Agric. Food Sci.* 28, 70–83. <https://doi.org/10.23986/afsci.79329>.
- Kirchmann, H., Gerzabek, M.H., 1999. Relationship between soil organic matter and micropores in a long-term experiment at Ultima, Sweden. *J. Plant Nutr. Soil Sci.* 162, 493–498. [https://doi.org/10.1002/\(sici\)1522-2624\(199910\)162:5<493::aid-jpln493>3.0.co;2-s](https://doi.org/10.1002/(sici)1522-2624(199910)162:5<493::aid-jpln493>3.0.co;2-s).
- Koestel, J., Jorda, H., 2014. What determines the strength of preferential transport in undisturbed soil under steady-state flow. *Geoderma* 217, 144–160. <https://doi.org/10.1016/j.geoderma.2013.11.009>.
- Kopittke, P.M., Dalal, R.C., Hoeschen, C., Li, C., Menzies, N.W., Mueller, C.W., 2020. Soil organic matter is stabilized by organo-mineral associations through two key processes: the role of the carbon to nitrogen ratio. *Geoderma* 357, 113974. <https://doi.org/10.1016/j.geoderma.2019.113974>.
- Kopittke, P.M., Hernandez-Soriano, M.C., Dalal, R.C., Finn, D., Menzies, N.W., Hoeschen, C., Mueller, C.W., 2018. Nitrogen-rich microbial products provide new organo-mineral associations for the stabilization of soil organic matter. *Glob. Chang. Biol.* 24, 1762–1770. <https://doi.org/10.1111/gcb.14009>.
- Lal, R., 2004. Soil carbon sequestration to mitigate climate change. *Geoderma* 123, 1–22. <https://doi.org/10.1016/j.geoderma.2004.01.032>.
- Larsbo, M., Koestel, J., Kätterer, T., Jarvis, N., 2016. Preferential transport in macropores is reduced by soil organic carbon. *Vadose Zone J.* 15, 1–7. <https://doi.org/10.2136/vzj2016.03.0021>.
- Leuther, F., Schlüter, S., 2021. Impact of freeze-thaw cycles on soil structure and soil hydraulic properties. *Soil* 7, 179–191. <https://doi.org/10.5194/soil-2021-13>.
- Liu, B., Fan, H., Jiang, Y., Renming, M., 2023. Evaluation of soil macro-aggregate characteristics in response to soil macropore characteristics investigated by X-ray computed tomography under freeze-thaw effects. *Soil Tillage Res.* 225. <https://doi.org/10.1016/j.still.2022.105559>.
- Ma, R., Cai, C., Li, Z., Wang, J., Xiao, T., Peng, G., Yang, W., 2015. Evaluation of soil aggregate microstructure and stability under wetting and drying cycles in two Ultisols using synchrotron-based X-ray micro-computed tomography. *Soil Tillage Res.* 149, 1–11. <https://doi.org/10.1016/j.still.2014.12.016>.
- Ma, R., Jiang, Y., Liu, B., Fan, H., 2021. Effects of pore structure characterized by synchrotron-based micro-computed tomography on aggregate stability of black soil under freeze-thaw cycles. *Soil Tillage Res.* 207, 104855. <https://doi.org/10.1016/j.still.2020.104855>.
- Madison, W.I., 2008. *Soil science glossary terms committee. Glossary of Soil Science Terms 2008*. Soil Science Society of America. ISBN 978-0-89118-851-3.
- Minasny, B., McBratney, A.B., 2018. Limited effect of organic matter on soil available water capacity. *Eur. J. Soil Sci.* 69, 39–47. <https://doi.org/10.1111/ejss.12475>.
- Otsu, N., 1979. A threshold selection method from gray-level histograms. *IEEE Trans. Syst. Man Cyber.* 9, 62–66. <https://doi.org/10.1109/TSMC.1979.4310076>.
- Peele, T.C., Beale, O.W., 1941. Influence of microbiological activity upon aggregation and erodibility of Lateritic soils. *Soil Sci. Soc. Am. J.* 5, 33–35. <https://doi.org/10.2136/sssaj1941.0361599500050000C0005x>.
- Peng, J., Wu, X., Ni, S., Wang, J., Song, Y., Cai, C., 2022. Investigating intra-aggregate microstructure characteristics and influencing factors of six soil types along a climatic gradient. *Catena* 210, 105867. <https://doi.org/10.1016/j.catena.2021.105867>.
- Pittman, F., Mohammed, A., Cey, E., 2020. Effects of antecedent moisture and macroporosity on infiltration and water flow in frozen soil. *Hydrol. Process.* 34, 795–809. <https://doi.org/10.1002/hyp.13629>.
- Pöhlitz, J., Rücknagel, J., Schlüter, S., Vogel, H.J., Christen, O., 2019. Computed tomography as an extension of classical methods in the analysis of soil compaction, exemplified on samples from two tillage treatments and at two moisture tensions. *Geoderma* 346, 52–62. <https://doi.org/10.1016/j.geoderma.2019.03.023>.
- Rabot, E., Wiesmeier, M., Schlüter, S., Vogel, H.J., 2018. Soil structure as an indicator of soil functions: a review. *Geoderma* 314, 122–137. <https://doi.org/10.1016/j.geoderma.2017.11.009>.
- Ramírez-Flores, J.C., Woche, S.K., Bachmann, J., Goebel, M.O., Hallett, P.D., 2008. Comparing capillary rise contact angles of soil aggregates and homogenized soil. *Geoderma* 146, 336–343. <https://doi.org/10.1016/j.geoderma.2008.05.032>.
- Rasa, K., Horn, R., Rätty, M., Yli-Halla, M., Pietola, L., 2009. Shrinkage properties of differently managed clay soils of Finland. *Soil Use Manag.* 25, 175–182. <https://doi.org/10.1111/j.1475-2743.2009.00214.x>.
- Rasa, K., Pennanen, T., Peltoniemi, K., Velmala, S., Fritze, H., Kaseva, J., Joona, J., Uusitalo, R., 2021. Pulp and paper mill sludges decrease soil erodibility. *J. Environ. Qual.* 50, 172–184. <https://doi.org/10.1002/jeq2.20170>.
- Rätty, M., Termonen, M., Soinne, H., Nikama, J., Rasa, K., Lappalainen, R., Auvinen, H., Keskinen, R., 2023. Improving coarse-textured mineral soils with pulp and paper mill sludges: functional considerations at laboratory scale. *Geoderma* 438. <https://doi.org/10.1016/j.geoderma.2023.116617>.
- Rawls, W.J., Pachepsky, Y.A., Ritchie, J.C., Sobecki, T.M., Bloodworth, H., 2003. Effect of soil organic carbon on soil water retention. *Geoderma* 116, 61–76. [https://doi.org/10.1016/S0016-7061\(03\)00094-6](https://doi.org/10.1016/S0016-7061(03)00094-6).
- Schmidt, M.W., Torn, M.S., Abiven, S., Dittmar, T., Guggenberger, G., Janssens, I.A., Kleber, M., Kögel-Knabner, I., Lehmann, J., Manning, D.A., Nannipieri, P., 2011. Persistence of soil organic matter as an ecosystem property. *Nature* 478, 49–56. <https://doi.org/10.1038/nature10386>.
- Soille, P., 2004. *Morphological Image Analysis - Principles and Applications, Second Edition*. Springer-Verlag, Berlin Heidelberg New York. ISBN 3-540-42988-3.
- Soinne, H., Keskinen, R., Tähtikarhu, M., Kuva, J., Hyväluoma, J., 2023. Effects of organic carbon and clay contents on structure-related properties of arable soils with high clay content. *Eur. J. Soil Sci.* 74, e13424. <https://doi.org/10.1111/ejss.13424>.
- Thangarajan, R., Bolan, N.S., Tian, G., Naidu, R., Kunhikrishnan, A., 2013. Role of organic amendment application on greenhouse gas emission from soil. *Sci. Total Environ.* 465, 72–96. <https://doi.org/10.1016/j.scitotenv.2013.01.031>.
- Turtola, E., Alakukku, L., Uusitalo, R., Kaseva, J., 2007. Surface runoff, subsurface drainflow and soil erosion as affected by tillage in a clayey Finnish soil. *Agric. Food Sci.* 16, 332–351. <https://doi.org/10.2137/14596607784125429>.
- Turunen, M., Hyväluoma, J., Heikkinen, J., Keskinen, R., Kaseva, J., Hannula, M., Rasa, K., 2020. Quantifying the pore structure of different biochars and their impacts on the water retention properties of Sphagnum moss growing media. *Biosyst. Eng.* 191, 96–106. <https://doi.org/10.1016/j.biosystemseng.2020.01.006>.
- Uusitalo, R., Ylivainio, K., Hyväluoma, J., Rasa, K., Kaseva, J., Nylund, P., Pietola, L., Turtola, E., 2012. The effects of gypsum on the transfer of phosphorus and other nutrients through clay soil monoliths. *Agric. Food Sci.* 21, 260–278. <https://doi.org/10.23986/afsci.4855>.
- Vogel, C., Mueller, C.W., Hoeschen, C., Buegger, F., Heister, K., Schulz, S., Schlotter, M., Kögel-Knabner, I., 2014. Submicron structures provide preferential spots for carbon and nitrogen sequestration in soils. *Nat. Commun.* 5, 2947. <https://doi.org/10.1038/ncomms3947>.
- Winstone, B.C., Heck, R.J., Munkholm, L.J., Deen, B., 2019. Characterization of soil aggregate structure by virtual erosion of X-ray CT imagery. *Soil Tillage Res.* 185, 70–76. <https://doi.org/10.1016/j.still.2018.09.001>.

- Yu, X., Wu, C., Fu, Y., Brookes, P.C., Lu, S., 2016. Three-dimensional pore structure and carbon distribution of macroaggregates in biochar-amended soil. *Eur. J. Soil Sci.* 67, 109–120. <https://doi.org/10.1111/ejss.12305>.
- Zhang, H., He, H., Gao, Y., Mady, A., Filipović, V., Dyck, M., Lv, J., Liu, Y., 2023. Applications of computed tomography (CT) in environmental soil and plant sciences. *Soil Tillage Res.* 226. <https://doi.org/10.1016/j.still.2022.105574>.
- Zhou, H., Chen, C., Wang, D., Arthur, E., Zhang, Z., Guo, Z., Peng, X., Mooney, S.J., 2020. Effect of long-term organic amendments on the full-range soil water retention characteristics of a Vertisol. *Soil Tillage Res.* 202, 104663 <https://doi.org/10.1016/j.still.2020.104663>.
- Zibilske, L.M., Clapham, W.M., Rourke, R.V., 2000. Multiple applications of paper mill sludge in an agricultural system: soil effects. *J. Environ. Qual.* 29, 1975–1981. <https://doi.org/10.2134/jeq2000.00472425002900060034x>.